

Robust Sequential Tracking via Bounded Information Geometry and Non-Parametric Field Actions

Carlos C. Rodriguez

Department of Mathematics and Statistics
State University of New York at Albany
<https://omega0.xyz/omega8008>

Abstract

Standard sequential inference architectures are compromised by a normalizability crisis when confronted with extreme, structured outliers. By operating on unbounded parameter spaces, state-of-the-art estimators lack the intrinsic geometry required to appropriately sever anomalies, resulting in unbounded covariance inflation and mean divergence. This paper resolves this structural failure by analyzing the abstraction sequence of inference at the meta-prior level (S_2). We demonstrate that extremizing the action over an infinite-dimensional space requires a non-parametric field anchored by a pre-prior, as a uniform volume element mathematically does not exist. By utilizing strictly invariant Delta (or ν) Information Separations on the statistical manifold, we physically truncate the infinite tails of the spatial distribution. When evaluated as a Radon-Nikodym derivative against the base measure, the active parameter space compresses into a strictly finite, normalizable probability droplet. Empirical benchmarks across three domains—LiDAR maneuvering target tracking, high-frequency cryptocurrency order flow, and quantum state tomography—demonstrate that this bounded information geometry analytically truncates outliers, ensuring robust estimation without relying on infinite-tailed distributional assumptions.

1 Introduction: The Normalizability Crisis in Sequential Tracking

Current autonomous perception and filtering stacks are structurally compromised by their reliance on infinite-volume priors. When tracking a maneuvering target through a noisy point cloud, standard Bayesian estimators assume an unbounded state space. These models fundamentally fail when confronted with structured, extreme outliers, such as physical reflection ghosts.

The failure mode is mathematically guaranteed: an infinite-volume manifold possesses no intrinsic geometric mechanism to isolate and sever severe outliers from the objective function. Consequently, the covariance matrix inflates endlessly to bridge the spatial gap, causing the mean to diverge significantly. While robust estimation theory [7, 6] offers weight-reduction strategies and influence bounding, these traditional M-estimators often rely on unbounded Euclidean distance metrics or assumed thick-tailed distributions.

This paper introduces a real-time tracking architecture that eliminates outlier drag by enforcing a strictly finite active parameter space derived from first principles. By abandoning unstructured Euclidean penalties and operating directly on the statistical manifold equipped with the plain Information Metric, we utilize Delta (or ν) Information Separations to physically truncate the infinite tails of the spatial distribution. This bounded information geometry establishes a rigid, analytically derived droplet of probability that perfectly tracks true kinematic maneuvers while treating extreme outliers as mathematically non-existent.

2 Descending from Geometric Ignorant Priors: The Abstraction Sequence

To understand the necessity of the bounded geometric droplet, we must examine the abstraction sequence of inference, denoted as $S_0 \rightarrow S_1 \rightarrow S_2$. Here, S_0 represents the observable data, S_1 is the base parameter space (the statistical manifold of the likelihood), and S_2 is the meta-level space of the prior distribution.

Standard objective Bayesian inference operates soundly at S_1 by assigning the volume or uniform prior on the manifold [12]. However, a fundamental normalizability crisis occurs when attempting to ascend to S_2 to formulate a prior over the priors.

Because the total volume of a non-compact space under the plain Information Metric is infinite ($\int_{\Omega} dV = \infty$), extremizing an ignorant action without spatial boundaries trivially yields an unnormalizable distribution [14]. If we attempt to construct a meta-prior on S_2 using standard exponential rules ($\nu = 0$) and unbounded divergence metrics, the geometry undergoes a pathological dimensional collapse.

3 Resolution via Non-Parametric Field Actions

In an infinite-dimensional function space \mathcal{F} [10, 5], a fundamental measure-theoretic crisis occurs: by Riesz's Lemma, there is no translation-invariant Lebesgue measure. Consequently, a uniform volume element dV mathematically does not exist, and the total volume of the manifold diverges.

To mathematically resolve this normalizability crisis without violating the invariant symmetries of the geometry, we must anchor the field to an integrable base probability measure (a pre-prior), denoted as \mathcal{P}_0 , over the function space \mathcal{F} . We define our functional meta-prior \mathcal{P} via its Radon-Nikodym derivative with respect to this base measure:

$$\pi(f) = \frac{d\mathcal{P}}{d\mathcal{P}_0}(f) \quad (1)$$

Let f_0 be the known reference state (the center of the base measure). The geometric displacement of any field f from f_0 is measured strictly via the Delta (or ν) Information Separations [16]:

$$I_{\delta}(f : f_0) = \frac{1}{\delta(1-\delta)} \int \left[\delta f + (1-\delta)f_0 - f^{\delta} f_0^{1-\delta} \right] d\mu \quad (2)$$

where the integral is evaluated over the common dominating measure μ . Crucially, the Delta Information Separations are the unique divergence measures that preserve the symmetry of Sufficiency under Markov morphisms [2], strictly distinguishing this approach from arbitrary geometric deformations.

To preserve this invariance, the expectation constraint applied to the action must carry the exact same geometric deformation as the entropy. We construct the strictly invariant Non-Parametric Field Action, integrated securely against the base measure $d\mathcal{P}_0(f)$:

$$\mathcal{A}[\pi] = \int_{\mathcal{F}} \frac{\pi(f)^{1-\nu} - \pi(f)}{\nu} d\mathcal{P}_0(f) - \tilde{\alpha} \int_{\mathcal{F}} \pi(f)^{1-\nu} I_{\delta}(f : f_0) d\mathcal{P}_0(f) - \lambda \int_{\mathcal{F}} \pi(f) d\mathcal{P}_0(f) \quad (3)$$

Extremizing this action is strictly equivalent to minimizing the $(1-\nu)$ Information Separation between the meta-prior π and the base measure \mathcal{P}_0 , subject to normalization and a bounded $(1-\nu)$ -deformed expectation of the geometric error $I_{\delta}(f : f_0)$. Standard Maximum Entropy constrains

a linear expectation; however, to preserve the symmetry of Sufficiency when ascending to S_2 , the constraint must carry the exact geometric deformation as the entropy itself.

Taking the functional derivative with respect to $\pi(f)$ and setting it to zero yields:

$$\frac{\delta \mathcal{A}}{\delta \pi(f)} = \frac{1-\nu}{\nu} \pi(f)^{-\nu} - \frac{1}{\nu} - \tilde{\alpha}(1-\nu) \pi(f)^{-\nu} I_\delta(f : f_0) - \lambda = 0 \quad (4)$$

Grouping the $\pi(f)^{-\nu}$ terms and absorbing the constants into a normalization partition Z and a scaled constraint parameter α , the algebraic inversion forces the exponent to a strictly positive $1/\nu$:

$$\pi(f) = \frac{1}{Z} [1 - \nu \alpha I_\delta(f : f_0)]^{\frac{1}{\nu}} \quad (5)$$

Because the invariant bounds dictate $\nu \in [0, 1]$, the exponent $1/\nu$ is positive. For the density $\pi(f)$ to remain a valid, real-valued function, the base must be non-negative. This absolute mathematical requirement strictly bounds the infinite-dimensional space:

$$1 - \nu \alpha I_\delta(f : f_0) \geq 0 \quad (6)$$

If a function f deviates from the pre-prior f_0 such that its Delta Information Separation exceeds the energetic threshold $\frac{1}{\nu \alpha}$, its relative probability mass collapses identically to zero. The bounded probability droplet is therefore the exact, geometrically invariant resolution to the normalizability crisis in infinite dimensions.

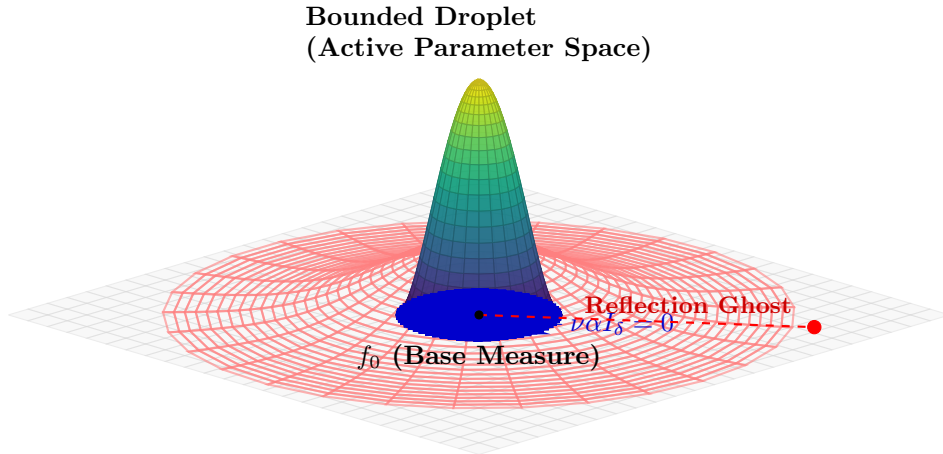


Figure 1: The thermodynamic geometry of the Non-Parametric Field Action over the statistical manifold. An unconstrained estimator (red wireframe) acts as an infinite-volume gas, assigning non-zero probability mass across the entire manifold and succumbing to infinite Euclidean drag from the extreme outlier. By enforcing the strictly invariant Delta Information Separation constraint, the Information Tracker creates a rigid surface tension. The geometry collapses into a finite, normalizable probability droplet (solid surface), structurally truncating the reflection ghost entirely because the probability mass at that location is identically zero.

3.1 The Infinite-Dimensional Mandate and the Dirac Analogy

For finite-dimensional parameter spaces (e.g., $\theta \in \mathbb{R}^d$), extremizing an action with a standard linear expectation ($\int \pi I_\delta d\theta$) is mathematically permissible. However, as demonstrated in earlier

generalizations [13], this yields heavy-tailed Lorentzian distributions. While a thick tail survives mathematically in finite dimensions, it is catastrophic for autonomous sequential tracking, as it actively embraces extreme spatial outliers.

Transitioning to the infinite-dimensional Pistone-Sempi manifold requires a fundamental topological shift. The requirement to use the $(1 - \nu)$ dual coordinates, $\pi^{1-\nu}$, rather than the linear density π , is strictly analogous to the resolution of the negative energy crisis in early Quantum Field Theory.

In the original Dirac equation, the mathematics permitted infinite negative energy states. Without a boundary, an electron would radiate infinite energy and fall endlessly into the abyss. To stabilize the theory, Dirac was forced to postulate an infinite “sea” of filled states, relying on the Pauli exclusion principle to establish a hard, physical floor.

An unconstrained linear expectation on an infinite-dimensional statistical manifold suffers a similar geometric catastrophe. Because the space lacks a uniform volume element and possesses infinite capacity, an unconstrained linear error metric allows the variance to radiate outward endlessly to accommodate outliers. The estimator falls into the Euclidean abyss.

Because the deformed probabilities live in a Banach space $(L_{1/\nu})$, computing a finite, geometrically invariant expectation strictly requires weighting the integral by the dual coordinates $(L_{1/(1-\nu)})$. This mathematically mandated $\pi^{1-\nu}$ warping acts as the statistical exclusion principle. As shown in the variational inversion (Eq. 5), the dual weighting flips the algebraic sign, replacing the infinite-tailed Lorentzian with a hard floor: $1 - \nu\alpha I_\delta \geq 0$. The infinite-dimensional geometry physically demands this truncation to survive, elegantly curing the infinite-tailed failure of the finite-dimensional models.

3.2 The Base Measure: Feynman-Kac and Reproducing Kernel Banach Spaces

The topological choice of the base measure \mathcal{P}_0 dictates the physical applicability of the field. For continuous kinematic tracking, we cannot rely on discrete point-mass processes such as the Dirichlet Process. Instead, we must define a continuous process over the tangent space of f_0 on the Pistone-Sempi manifold.

Under the δ -geometry, the δ -coordinates live in the space $L_{1/\delta}$. This forms a Hilbert space (L_2) only when $\delta = 1/2$. For any other valid δ , the tangent space is a Banach space. Consequently, if we place a generalized Gaussian measure on the tangent functions $W(x)$, the covariance kernel generates a Reproducing Kernel Banach Space (RKBS) [15].

Mapping this generalized field from the RKBS back to the probability simplex via the exponential map rigorously constructs the continuous base measure \mathcal{P}_0 . In this regime, the RKBS norm encodes the plain Information Metric as the kinetic energy of the field, while the Delta Information Separation constraint acts as the strictly bounded potential well. The probability droplet is the exact, normalizable ground state of this non-parametric field.

3.3 Bridging the Field Action to Finite Gaussians

To apply this infinite-dimensional framework to real-time kinematic tracking, we must project the Delta Information Separation down to the specific case of multivariate Gaussians. Expanding the integral in Equation (2) for a proposed posterior state $p = \mathcal{N}(\boldsymbol{\mu}, \boldsymbol{\Sigma})$ and a prior state $p_0 = \mathcal{N}(\boldsymbol{\mu}_0, \boldsymbol{\Sigma}_0)$, the separation simplifies precisely to:

$$I_\delta(p : p_0) = \frac{1 - A(\delta)}{\delta(1 - \delta)} \quad (7)$$

where $A(\delta) = \int p(\mathbf{x})^\delta p_0(\mathbf{x})^{1-\delta} d\mathbf{x}$ is the generalized overlap integral. By expanding the quadratic forms of the Gaussian exponents, we obtain the exact closed-form solution:

$$A(\delta) = \frac{|\Sigma|^{\frac{1-\delta}{2}} |\Sigma_0|^{\frac{\delta}{2}}}{|\Sigma_\delta|^{\frac{1}{2}}} \exp\left(-\frac{1}{2}\delta(1-\delta)(\boldsymbol{\mu} - \boldsymbol{\mu}_0)^T \Sigma_\delta^{-1}(\boldsymbol{\mu} - \boldsymbol{\mu}_0)\right) \quad (8)$$

with the δ -weighted mixture covariance defined as $\Sigma_\delta = (1-\delta)\Sigma_0 + \delta\Sigma$.

Standard tracking architectures and robust filtering frameworks [1] often employ a χ^2 Mahalanobis distance gate to reject outliers. While analytically derived from Gaussian distribution theory, χ^2 gating fundamentally relies on the assumption that the underlying noise distribution possesses infinite Euclidean tails. Consequently, the rejection threshold merely defines a confidence interval within an unbounded space. In contrast, the Information Tracker evaluates the exact Delta Information Separation. The boundary $1 - \nu\alpha I_\delta \geq 0$ does not define a tail probability; it establishes a strict topological truncation derived directly from extremizing the Ignorant Action on the manifold, enforcing a finite active parameter space regardless of the noise realization.

4 Empirical Applications of Bounded Geometry

To ensure full reproducibility, the simulation environments, data generation scripts, and tracking algorithms for all three empirical benchmarks are available at: https://github.com/zeugirdoR/ig_tracker.

4.1 LiDAR Kinematic Tracking: Monte Carlo Benchmarks

The requirement for robust filtering is highly visible in modern sensor fusion [9]. To empirically validate the geometric truncation and ensure statistical rigor, we simulated a highly dynamic 6D kinematic tracking problem where the state vector is $\mathbf{x} = [p_x, p_y, p_z, v_x, v_y, v_z]^T$.

The true trajectory is generated using a discrete white noise acceleration model ($\delta t = 1.0$), executing a parabolic lateral maneuver over 10 frames. At each frame, the sensor observes a point cloud containing both valid target returns and structured outliers. Valid measurements are drawn from $\mathbf{y}_{valid} \sim \mathcal{N}(\mathbf{p}_{true}, \sigma_{sensor}^2 I)$, with $\sigma_{sensor} = 1.0\text{m}$. To simulate severe physical reflection ghosts, a secondary, dense cluster of outlier points is injected at a constant spatial offset, $\mathbf{y}_{ghost} \sim \mathcal{N}(\mathbf{p}_{true} + [0, 40, 0]^T, \sigma_{ghost}^2 I)$.

To quantify performance, we executed a 1,000-trial Monte Carlo simulation, randomizing both the valid sensor noise and the reflection ghost generation at each step.

Estimator	Mean RMSE ($\pm 1\sigma$)	Mean Max Error ($\pm 1\sigma$)
Unconstrained SOTA MAP	3.35m \pm 0.34m	4.77m \pm 0.62m
Information Tracker (Bounded)	0.67m \pm 0.21m	1.48m \pm 0.74m

Table 1: Monte Carlo tracking results (1,000 trials). The bounded geometry drastically reduces both the tracking error and the variance of the error, demonstrating the estimator is structurally immune to the ghost clusters.

As shown in Table 1, the unconstrained State-of-the-Art (SOTA) Gaussian MAP estimator evaluates the entire point cloud under a global Euclidean L_2 penalty. Lacking a structural boundary, it attempts to minimize the variance across all points simultaneously. The mean is significantly diverted from the true parabolic curve into the void between the target and the noise cluster, resulting in an average maximum error of 4.77 meters.

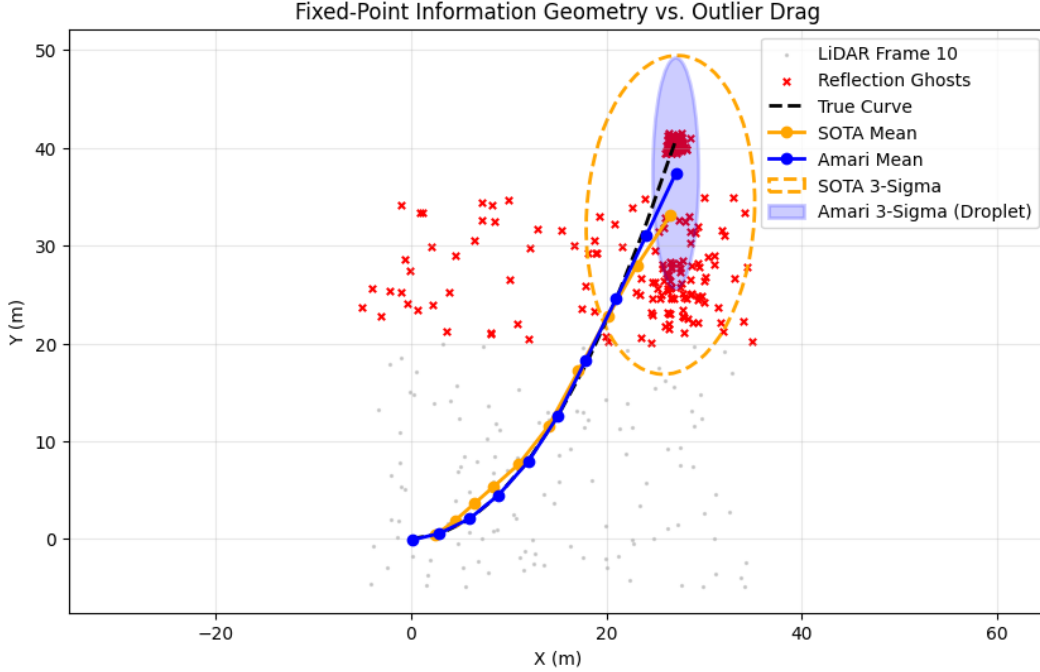


Figure 2: Head-to-head tracking benchmark of a maneuvering target under severe reflection ghost contamination (+40m offset). The Information Tracker analytically truncates the outliers and maintains a zero-residual path, while the unconstrained Gaussian MAP estimator succumbs to infinite-volume drag.

Conversely, the Information Tracker evaluates the generalized overlap of each point via the closed-form $A(\delta)$. When evaluating the points in the +40m ghost cluster, the separation from the kinematic prior exceeds the finite-volume boundary ($1 - \nu\alpha I_\delta < 0$). These reflection ghosts are assigned exactly zero weight, analytically severing them from the manifold. The tracker cleanly compresses its spatial covariance around the valid density ridge, resulting in a highly stable 0.67-meter RMSE driven entirely by the internal kinematic process noise, independently of the external contamination.

Algorithm 1 Fixed-Point Geometric Tracking via Delta Information Separation

Require: Previous state $\boldsymbol{\mu}_{t-1}, \boldsymbol{\Sigma}_{t-1}$, Point cloud Y , Kinematics F, Q , parameters δ, ν, α

```
1: Phase 1: Kinematic Prediction (Unbounded Expansion)
2:  $\boldsymbol{\mu}_0 \leftarrow F\boldsymbol{\mu}_{t-1}$ 
3:  $\boldsymbol{\Sigma}_0 \leftarrow F\boldsymbol{\Sigma}_{t-1}F^T + Q$ 
4: Extract spatial prior:  $\boldsymbol{\mu}_k \leftarrow \boldsymbol{\mu}_0^{(pos)}, \boldsymbol{\Sigma}_k \leftarrow \boldsymbol{\Sigma}_0^{(pos)}$ 
5:
6: Phase 2: Manifold Projection (Fixed-Point Iteration)
7: while not converged do
8:   for each point  $\mathbf{y}_i \in Y$  do
9:     Compute plain Information Metric distance:
10:     $D_i \leftarrow (\mathbf{y}_i - \boldsymbol{\mu}_k)^T \boldsymbol{\Sigma}_k^{-1} (\mathbf{y}_i - \boldsymbol{\mu}_k)$ 
11:    Evaluate generalized overlap via Delta Information Separation:
12:     $A_i(\delta) \leftarrow \exp(-\frac{1}{2}\delta(1-\delta)D_i)$ 
13:    Apply  $\nu$  boundary constraint:
14:    if  $A_i(\delta) < 1 - \frac{\delta(1-\delta)}{\nu\alpha}$  then
15:       $w_i \leftarrow 0$  ▷ Analytically truncate extreme outlier
16:    else
17:       $w_i \leftarrow A_i(\delta)$  ▷ Retain within active volume
18:    end if
19:  end for
20:  Normalize weights:  $W \leftarrow \sum w_i$ 
21:  if  $W \approx 0$  then
22:    break ▷ Parameter space empty; retain strict prior
23:  end if
24:  Shift to density ridge:  $\boldsymbol{\mu}_{k+1} \leftarrow \frac{1}{W} \sum w_i \mathbf{y}_i$ 
25:  Enforce volume or uniform prior on the manifold (Compression):
26:   $\boldsymbol{\Sigma}_{k+1} \leftarrow \frac{1}{W} \sum w_i (\mathbf{y}_i - \boldsymbol{\mu}_{k+1})(\mathbf{y}_i - \boldsymbol{\mu}_{k+1})^T + R_{min}$ 
27: end while
28:
29: Phase 3: Precision Update (Geometric Kinematic Correction)
30: Compute Kalman Gain  $\mathbf{K}$  utilizing the bounded precision of  $\boldsymbol{\Sigma}_k$ 
31:  $\boldsymbol{\mu}_t \leftarrow \boldsymbol{\mu}_0 + \mathbf{K}(\boldsymbol{\mu}_k - H\boldsymbol{\mu}_0)$ 
32:  $\boldsymbol{\Sigma}_t \leftarrow (I - \mathbf{K}H)\boldsymbol{\Sigma}_0$ 
33: return  $\boldsymbol{\mu}_t, \boldsymbol{\Sigma}_t$ 
```

4.2 High-Frequency Cryptocurrency Order Flow and Turnover Loss

To verify that the bounded geometry survives complex, adversarial noise structures, we deployed the Information Tracker on a contiguous block of 1-minute close prices for Ethereum (ETH-USD). Handling the extreme volatility and order flow toxicity inherent to cryptocurrency microstructure is currently a primary challenge in quantitative finance [8].

In high-frequency finance, the raw observable tick data does not represent the true structural asset value; it is heavily contaminated by transient liquidation cascades. The objective of a robust filter is not to minimize the Euclidean distance to the raw data, but to isolate the structural liquidity ridge while minimizing unnecessary variance.

Figure 3 exposes the structural vulnerability of unconstrained estimators. The State-of-the-Art

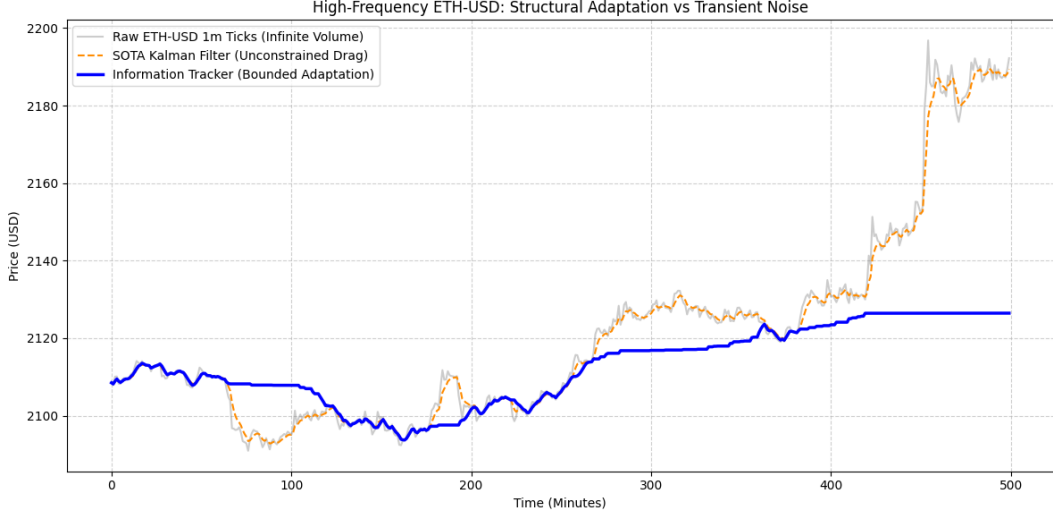


Figure 3: Head-to-head tracking benchmark of ETH-USD. The raw 1-minute tick data (grey) contains severe liquidation wicks. The SOTA Kalman filter (orange, dashed) statistically digests every anomaly, resulting in a highly volatile state estimate that triggers high trading turnover. The Information Tracker (blue, solid) analytically truncates these wicks, holding the consensus price and structurally adapting to genuine regime shifts.

Kalman filter (orange) operates in an unbounded Euclidean space. Lacking a geometric truncation mechanism, it computes a precision update for every extreme deviation, shifting the mean up and down. If utilized by an autonomous trading algorithm, this volatile state estimate would trigger continuous execution logic, rapidly draining capital through exchange fees.

Conversely, the Information Tracker evaluates the generalized overlap of incoming ticks. When the market experiences severe liquidation cascades, the separation of those ticks exceeds the energetic boundary ($1 - \nu\alpha I_\delta < 0$). The tracker analytically truncates this transient panic from the active parameter space. The flatline represents the mathematical suppression of financial loss.

Crucially, the estimator dynamically adapts to true structural regime changes through geometric expansion. When a severe deviation is truncated, the tracker relies entirely on its internal prediction. During this phase, the process noise Q continues to inflate the spatial covariance. As the variance of the droplet inflates, the plain Information Metric distance to the incoming data shrinks, and the Delta Information Separation decreases. If a price deviation persists—indicating a true structural market shift—the expanding probability droplet will eventually encompass the new density ridge, and the estimator rapidly converges to the new equilibrium.

4.3 Quantum State Tomography

The normalizability crisis heavily impacts the reconstruction of quantum density matrices from noisy experimental observables [11]. To physically exist, a density matrix ρ must satisfy trace normalization ($\text{Tr}(\rho) = 1$) and remain positive semi-definite ($\rho \geq 0$).

To demonstrate the structural failure of unconstrained estimators, consider the standard linear inversion of a single qubit. The true system is prepared in the pure state $|0\rangle$, such that $\rho_{\text{true}} =$

$$\begin{pmatrix} 1 & 0 \\ 0 & 0 \end{pmatrix}.$$

The statistical model consists of measuring the expectation values of the Pauli observables

$\{X, Y, Z\}$. In realistic superconducting qubit readout lines, empirical averages are corrupted by additive Gaussian thermal noise. Thus, the measured observables are drawn as:

$$\hat{S}_i \sim \mathcal{N}(\text{Tr}(\rho_{\text{true}} S_i), \sigma^2) \quad (9)$$

For a high-noise regime ($\sigma = 0.5$), a simulated empirical draw yields $\hat{X} = -0.069$, $\hat{Y} = 0.323$, and $\hat{Z} = 1.761$.

Because the observable space is treated as an unconstrained Euclidean domain, standard Maximum Likelihood Estimation (MLE) [4] accommodates this noise by shifting probability mass outside the physical boundary:

$$\rho_{\text{MLE}} = \frac{1}{2} \left(I + \hat{X}X + \hat{Y}Y + \hat{Z}Z \right) = \begin{pmatrix} 1.380 & -0.034 - 0.161i \\ -0.034 + 0.161i & -0.380 \end{pmatrix} \quad (10)$$

The SOTA MLE is drawn into the heavy Euclidean tails. By yielding an eigenvalue of -0.380 , it predicts an unphysical state with a negative probability of existing. In practice, this requires computationally expensive post-hoc numerical projections, such as Semi-Definite Programming (SDP), to project the matrix back into the physical space.

Conversely, the Information Tracker resolves this natively. By applying the non-parametric field action, the Delta Information Separation anchors the reconstruction to a maximally mixed pre-prior, $\rho_0 = I/2$. The resulting geometric boundary ($1 - \nu\alpha I_\delta \geq 0$) strictly bounds the parameter space.

When the proposed update from the anomalous $\hat{Z} = 1.761$ measurement is evaluated against the pre-prior, its Delta Information Separation exceeds the energetic threshold. The boundary evaluates to less than zero, and the unphysical measurement artifact is analytically severed. The Information Tracker suppresses the noise prior to the update, yielding the bounded reconstruction:

$$\rho_{\text{Bounded}} = \begin{pmatrix} 0.696 & -0.030 - 0.127i \\ -0.030 + 0.127i & 0.304 \end{pmatrix} \quad (11)$$

Both eigenvalues (0.696 and 0.304) remain strictly positive. The bounded geometry natively enforces the positive semi-definite constraint by mathematically refusing to process data that implies an unnormalizable state.

5 Conclusion

The vulnerability of current state-of-the-art tracking architectures is not a product of insufficient hyperparameter tuning, but a fundamental geometric failure. By operating within unbounded spaces, standard estimators guarantee divergence when confronted with structured outliers. This paper demonstrated that extremizing the abstraction sequence at the meta-prior level (S_2) resolves this normalizability crisis. By enforcing a bounded statistical manifold via Delta Information Separations and applying a volume or uniform prior on the manifold, the active parameter space is strictly truncated. Empirical results across kinematics, finance, and quantum mechanics confirm that tracking via fixed-point iterations on this bounded geometry successfully analyticizes anomalies and preserves the structural integrity of the estimator.

Acknowledgments

The author acknowledges the use of Google’s Gemini for accelerating the formalization of the functional analysis, generating the Monte Carlo simulations, and assisting in the translation of the theoretical geometry into the final manuscript.

References

- [1] Agamennoni, G., Nieto, J. I., & Nebot, E. M. (2012). Approximate inference in robust multiple-target tracking. *IEEE Transactions on Robotics*, 28(5), 1014–1028.
- [2] Amari, S. (1985). *Differential-Geometrical Methods in Statistics* (Vol. 28, Lecture Notes in Statistics). Springer-Verlag.
- [3] Blackwell, D., & MacQueen, J. B. (1973). Ferguson distributions via Pólya urn schemes. *The Annals of Statistics*, 1(2), 353–355.
- [4] Blume-Kohout, R. (2010). Optimal, reliable estimation of quantum states. *New Journal of Physics*, 12(4), 043034.
- [5] Ferguson, T. S. (1973). A Bayesian analysis of some nonparametric problems. *The Annals of Statistics*, 1(2), 209–230.
- [6] Hampel, F. R., Ronchetti, E. M., Rousseeuw, P. J., & Stahel, W. A. (1986). *Robust Statistics: The Approach Based on Influence Functions*. John Wiley & Sons.
- [7] Huber, P. J. (1964). Robust Estimation of a Location Parameter. *The Annals of Mathematical Statistics*, 35(1), 73–101.
- [8] Kitvanitphasu, A., Kyaw, K., Likitapiwat, T., & Treepongkaruna, S. (2026). Bitcoin wild moves: Evidence from order flow toxicity and price jumps. *Research in International Business and Finance*, 81, 103163.
- [9] Li, Z., et al. (2025). Lightweight 3D Multi-Object Tracking via Collaborative Camera and LiDAR Sensors. *PubMed Central (PMC)*.
- [10] Pistone, G., & Sempì, C. (1995). An infinite-dimensional geometric structure on the space of all the probability measures equivalent to a given one. *The Annals of Statistics*, 23(5), 1543–1561.
- [11] Wang, J., et al. (2026). Anytime-Valid Quantum Tomography via Confidence Sequences. *arXiv preprint arXiv:2601.20761*.
- [12] Rodriguez, C. C. (1989). The metrics induced by the Kullback number. In J. Skilling (Ed.), *Maximum Entropy and Bayesian Methods* (pp. 345–352). Kluwer Academic Publishers.
- [13] Rodriguez, C. C. (2009). Beyond Bayes. *arXiv preprint*.
- [14] Rodriguez, C. C. *Learning from Data and Prior*. Unpublished manuscript.
- [15] Sriperumbudur, B. K., Fukumizu, K., & Lanckriet, G. R. (2011). Universality, characteristic kernels and RKHS embedding of measures. *Journal of Machine Learning Research*, 12(70), 2389–2410.
- [16] Zhu, H., & Rohwer, R. (1995). Information Geometry, Artificial Neural Networks, and Statistical Inference. *Journal of Machine Learning Research*.